

Thermal-Hydraulics Operation Parameters Modeling and Analysis of KLT-40S Reactor at Steady-State and Transient Condition using RELAP5-3D

Abednego Kristanto^{a,*}, Alexander Agung^a, Kutut Suryopratomo^a

^a Department of Nuclear Engineering and Engineering Physics, Faculty of Engineering, Universitas Gadjah Mada, Yogyakarta, Indonesia
E-mail: *a_agung@ugm.ac.id

Abstract— One of Floating Nuclear Power Plant (FNPP) designs in the world is currently being built by Russian Federation, named “Academic Lomonosov,” which uses two PWR types, KLT-40S as its power unit. However, too little information regarding its detailed technical specification is available, including its thermal-hydraulics parameters. The objective of this research is to create a thermal-hydraulic model of KLT-40S reactor core use RELAP5-3D and to predict fuel and cladding temperature value at the steady-state condition, and transient condition with a variety of primary coolant mass flow rate and pressure to simulate abnormal event within the reactor. The reactor thermal-hydraulic model is created by dividing 121 coolant channels in the actual nuclear fuel assemblies into two channels: one channel to simulate coolant flow in 120 fuel assemblies with average heat generation, and the other channel to simulate coolant flow in one fuel assembly with highest heat generation in the core. The fuel structure had solid cylinder geometry and made from ceramic-metal UO₂ dispersed in the inert silumin matrix. The fuel cladding is made from zirconium alloy. These fuel heat structures generate heat from fission reaction and are modelled as a heat source according to the reactor power technical data, i.e., 150 MWt. The reactor axial power distribution is approximated by cosine distribution. Operation parameter variation that represents the real reactor normal operation condition in this research is a variation that has flow loss coefficient value 8,000, radial power peaking factor 1.1, and axial power peaking factor 1.1 with axial power peaking located in the middle of the fuel rod. The fuel and cladding temperature value at the steady-state condition and several transient conditions are predicted in this research, and there is no temperature value that goes beyond the safety limit.

Keywords— floating nuclear power plant; KLT-40S; thermal-hydraulics; RELAP5-3D.

I. INTRODUCTION

The need to increase the usage of environment-friendly energy to support sustainable development requires reliable, flexible, low greenhouse gas emission and affordable energy sources. A new generation of Nuclear Power Plants (NPP) nowadays, has those features. One of the most interesting designs of NPP to be applied in an archipelagic country like Indonesia that has difficulties in building inter-island electric network and land acquisition problem is the Floating Nuclear Power Plant (FNPP). One of many FNPP designs in the world is named “Akademik Lomonosov,” which designed by a Russian’s OKBM Afrikantov. This FNPP design use two Pressurized Water Reactor (PWR) type reactor, KLT-40S as its power unit.

KLT-40S has very few information regarding its detail of technical specifications, including its thermal-hydraulics parameters. Most of the technical data used in this research based on the “KLT-40S Overview” [1]. The other studies regarding the thermal-hydraulic of KLT-40S have been done

with both experiment and computation methods [2-6]. However, these researches deal with thermal-hydraulic problems in a fuel assembly. Furthermore, thermal-hydraulics modeling and analysis of KLT-40S reactor to calculate fuel and cladding temperature during steady-state and transient (with a variation of pressure and coolant mass flow rate) condition at full power 150 MWt has not been done using RELAP5-3D code. Modeling and analysis of the reactor operation parameters are necessary to prove the specification data claimed by the designer and to establish safety regulation for this specific reactor. This research is modeling all fuel assemblies and fuel channels inside the reactor pressure vessel (RPV) of the KLT-40S reactor with RELAP5-3D code. The result of this research is expected to become the basis of other thermal-hydraulic analyses of the KLT-40S reactor.

The objectives of this research are to obtain a thermal-hydraulics model of the KLT-40S reactor core and to determine the fuel and cladding temperature at the steady and transient condition with a variety of primary coolant

pressure and mass flow rate to simulate abnormal events in the reactor. After the model is available, it could be used for further analysis of KLT-40S reactor safety. This research is limited only to the thermal hydraulics system inside the reactor pressure vessel. Thus, the reactor inlet will be modeled as a fluid source, and the reactor outlet will be modeled as a fluid container. Moreover, the reactor is assumed stationary; hence, the movement of the ship due to ocean waves is not modeled.

II. MATERIAL AND METHOD

A. Modeling of Hydrodynamics Components

Based on the reference [1], the KLT-40S reactor has the physical appearance, as shown in Fig. 1.

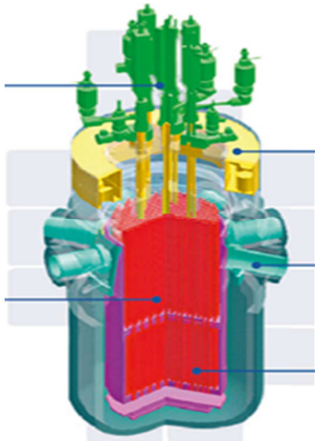


Fig. 1 Physical appearance of KLT-40S reactor [1]

The technical data of the KLT-40S reactor obtained from the reference [1] is summarized in Table 1.

TABLE I
TECHNICAL DATA OF KLT-40S REACTOR [1]

Parameter	Value
Reactor thermal power	150 MWt
Electric power, net	30 MWe
Efficiency	23.3 %
Primary coolant material	Light water (H ₂ O)
Moderator material	Light water (H ₂ O)
Reactor core height	1,200 mm
Fuel material	UO ₂ in an inert matrix
Fuel element geometry	Cylinder
Cladding material	Zircalloy
Fuel element outer diameter	6.8 mm
Number of fuel assemblies (FA) in a reactor core	121
Primary coolant mass flow rate	761 kg/s
Reactor operation pressure	12.7 MPa
Primary coolant at a core inlet temperature	280 °C
Primary coolant at a core outlet temperature	316 °C
RPV inner diameter	1,920 mm
RPV inner height	3,892 mm
RPV material	Russian Steel code 15Cr2NiMoVA-A

After the technical data is known, flow area in the heating channel, hydraulic diameter, flow geometry in the reactor

core, and axial heat generation distribution were calculated. Flow areas in the heating channel, hydraulic diameter, and flow geometry in the reactor core are calculated from the available technical data specification that available the reference [1]. Axial heat generation was approximated using cosine distribution, and calculated using the following equation:

$$q'(z) = q'_o \cos \frac{\pi z}{L_e} \quad (1)$$

where, q'_o is peak linear heat generation rate, L_e is extrapolation length where neutron flux has non zero value, and the value of z is in the range between $-L_e/2$ and $L_e/2$.

After the calculation has been done, thermal-hydraulic components of the KLT-40S reactor were nodalized to comply with RELAP-3D input requirements. The nodalization of the KLT-40S core components is shown in Fig. 2.

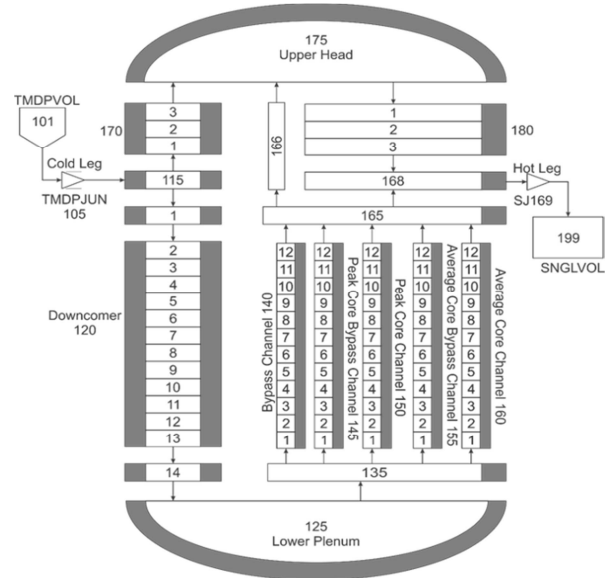


Fig. 2 Nodalization of KLT-40S thermal hydraulics components

This nodalization was then modeled into RELAP5-3D with the help of an interface software, SNAP. Figure 3 visualizes the nodalization in SNAP. Input requirement and nodalization of the component were made with the help of the software manual [7]. Component number 101 is a source volume to represents the fluid source which will enter the reactor. Operation pressure is set at 12.7 MPa, and the coolant temperature at reactor inlet is set at 280 °C or 553.15 K. Component 105 is a junction that connects the fluid source with other reactor thermal hydraulics components. At component 105, the value of coolant mass flow rate is set at 761 kg/s. Component 115 is the reactor inlet. The component with number 120 is an annulus channel, which represents the down comer region of the reactor. This channel is enclosed by reactor pressure vessel (RPV) steel in its outer diameter, and reactor barrel steel in its inner diameter. The down comer channel connects the coolant fluid to flow from the inlet to bottom region of the reactor,

represented by component 125. Component 125 wall is the bottom region of the reactor pressure vessel. From this bottom region, water coolant is flowing to the reactor core inlet which is represented by component number 135. Component 135 is modeled as a cylinder located at the bottom of the reactor core barrel.

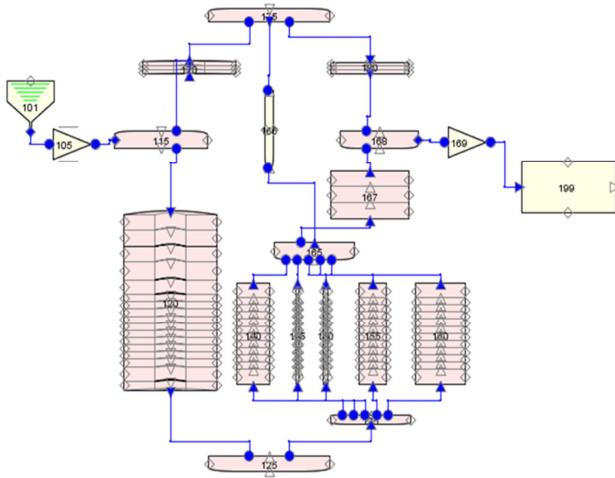


Fig. 3 KLT-40S reactor model in interface software, SNAP.

In the actual reactor core, the coolant from the core inlet will flow to the coolant channels inside the 121 nuclear fuel assemblies, and a bypass channel between core baffle and barrel that is represented by component 140. For simplification of the model, those 121 coolant channels in the reactor core are divided into two channels. One channel, which will represent the average heat generation channel (component 160), is formed by combining 120 channels, and one channel that represents the power peaking heat generation channel (component 150). The bypass channel at the middle of the fuel assemblies is modeled in the same way as the heating channel. A combined 120 bypass channels in the average heat generation channel is represented by component 155, and one bypass channel in the power peaking heat generation channel is represented by component 145.

The outlet of the five channels described above is connected to component 165, which represents the core outlet. Similar to component 135, component 165 is part of the reactor barrel and modeled as a cylinder. Component 167 represents the coolant channel above the core, and component 166 represents the control guide tube. The control guide tube can also be flowed by cooling fluid, assuming that all of the control rods are pulled out. Component 167 will flow the heated coolant from the core into the reactor outlet, which represented by component 168. Component 168 has the same vertical flow area as the reactor core barrel, but horizontally it is connected to junction 169 that represents the connection between the reactor system and another system outside the reactor pressure vessel. In this model, after the coolant fluid exiting from junction 169, the coolant fluid will be contained in component 199 that represents the fluid container. The geometry of component 199 is set to be very large with the purpose of keeping the pressure inside the container from affecting the pressure of systems in the reactor pressure vessel.

Besides the main thermal-hydraulics component described above, there are other components modeled in this research to approach the real flow condition in the reactor. Component 170 represents a small portion of the coolant that flows into the upper head of the reactor pressure vessel when the high-pressure fluid is entering the reactor. Component 175 receives the coolant flow from components 170 and 166; it represents the upper head of the reactor pressure vessel. The coolant fluid from component 175 then flows through empty volume inside the upper portion of the core barrel represented by component 180 before mix up with the heated fluid from the reactor core at reactor outlet or component 168.

B. Modeling of Heat Structure

After the hydrodynamics components that simulate the coolant flow inside the reactor is modeled, the next step is heat structure modeling of all the reactor structures. These structures are in direct contact with the coolant fluid. Therefore they give or take the heat from the fluid, then transfer it conductively from one channel into another. The first structure to be modeled is the reactor pressure vessel that is represented by heat structure 1201. This structure has a vertical cylinder geometry and uses Russian steel material with code 12Kh2NMFA [1]. Thermophysical properties of Russian steel material with code 12Kh2NMFA were taken from reference [8].

The upper and bottom structure of this pressure vessel in this model is represented by heat structure with number 1751 and 1251. These two structures are created with half-sphere geometry with a sphere fraction of 0.54 for heat structure 1751 and 0.434 for heat structure 1251. Heat structure 1751 and 1251 also use Russian steel material with code 15Kh2NMFA [1]. The reactor barrel in this model is represented by heat structure 1421 that has cylinder geometry and uses the same material as the reactor pressure vessel. This structure will transfer the heat that it takes from the fluid inside the reactor barrel conductively into its outside diameter. The reactor core baffle that is located inside the core barrel is represented by heat structure 1641. The geometry of heat structure 1641 is approached with the cylinder and use Russian steel with code 15Kh2NMFA as its material [1]. This structure will transfer the heat it takes from the fluid inside the reactor core into the outside of the baffle through conduction.

Heat structure number 1501 and 1601 represent fuel rods inside fuel assemblies. Heat structure 1501 represents the fuel rods inside a fuel assembly channel with power peaking heat generation. Heat structure 1601 represents all the fuel rods inside all other fuel assemblies that assumed to have an average value of heat generation in each of its fuel assemblies. These two structures have solid cylinder geometry and use ceramic-metal (cermet) UO₂ fuel dispersed in inert silumin matrix material and cladding material made from zirconium alloy (zircalloy) [1]. Thermophysical properties of fuel materials were taken from reference [8,9] for cermet UO₂ fuel dispersed in inert silumin matrix, and reference [10] for zircalloy.

These two structures are supposedly generating heat from the fission reaction inside the reactor, but in this research, the structure heat generation is modeled as heat generator

with the total power is set to an operating power known from the reference, which is 150 MW. A cosine distribution approximates the axial power distribution. The illustration of the axial power distribution of this KLT-40S reactor core model is shown in Fig. 4.

The difference between heat structure 1501 and 1601 is its number of fuel rods and the heat generation inside it. The number of fuel rods can be set by adjusting the heat transfer surface area between these two structures. Thus, the heat transfer surface area of heat structure 1601 is equal to 120 times the heat surface area of heat structure 1501. The same logic also applies to the determination of the power value generated in each structure. Conduction also takes place in the structure of bypass channels inside the fuel assemblies. These channel structures is represented by heat structure 1451 for the bypass channel inside the power peaking heat generation channel, and heat structure 1551 for the bypass channels inside the average heat generation channels. These two structures are modelled with same Russian steel material as the reactor pressure vessel and receives heat from the fluid inside heated channel in the fuel assemblies, then gives the heat to the fluid inside it.

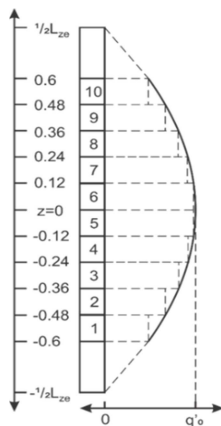


Fig. 4 Reactor core axial power distribution with the power peaking at the center of the fuel rod.

C. Simulation of Steady-State and Transient Condition

At steady-state condition, all reactor thermal hydraulics parameters are maintained to keep the constant turbine power generation. Based on that condition, the steady-state simulation will be done by running the calculation with constant operation parameter or constant coolant pressure and mass flow rate during the given simulation time. Hydrodynamics component modeling described above still has a problem because of unavailable friction coefficient data at each channel. This problem affects the coolant fluid mass flow distribution that will be different from the actual distribution. To resolve that problem, several variations of flow loss coefficient at the bypass channels will be used in the simulation and its effect on several axial and radial power peaking factors will be observed to determine which variation is the most suitable to represent the real coolant flow condition in the reactor core. Moreover, from the simulation at several power peaking factor variations, the optimum value of axial and radial power peaking factor at the power peaking heat generation channel can be determined and used in the transient simulation. The variation values of the flow loss coefficient are 0, 4,000,

8,000, 12,000, and 16,000. The variation value of axial and radial power peaking factor is 1.0 (homogeneous power distribution), 1.1, 1.2, and 1.3.

The resulting data from the steady-state simulation can be used to validate the RELAP5-3D model. Such validation is performed by comparing the steady-state simulation result with the available data taken from the reference. The aim of this validation is to make sure whether the simulation result from the RELAP5-3D code can be accepted or not. Reference [1] is used for this comparison. The parameters that were compared are the primary coolant temperature and mass flow rate at the outlet of the reactor.

The transient condition will happen if the reactor system that already on its steady-state condition is disturbed. The simulated disturbances in this research are disturbance caused by the change of coolant pressure and mass flow rate at the reactor inlet. This simulated transient will be done by giving the system input change that similar to step and ramp signal. This signal generation will start once the system has achieved its steady-state condition. With the data from the steady-state simulation, the exact time to start the parameters signal change generation will be known. In this research, the effect of each parameter change toward the system will be observed. Thus, the shift in pressure simulation and the change of mass flow rate simulation will be done separately and assumed independently at the reactor inlet. The shift in coolant pressure simulation will be done four times to simulate a 10% step increase, 10% step decrease, 10% ramp increase for 200 seconds, and 10% ramp decrease for 200 seconds. The value of a 10% pressure increase, and the decrease was based on acceptance criteria for transient in reference [11]. The change of coolant mass flow rate simulation will also be done four times to simulate a 20% step increase, a 20% step decrease, a 20% ramp increase for 200 seconds, and a 20% ramp decrease for 200 seconds. The value of 20% mass flow increase and the decrease was based on reference [12].

D. Result Analysis

The first result analysis is to determine the value of the flow loss coefficient at the bypass channels and axial and radial power peaking factor at the power peaking heat generation channel. This result will be used for later transient simulation. From this steady-state simulation, several data which will be taken are steam fraction at all of the fuel channels, steam fraction total at the outlet of the reactor, mass flow rate at all fuel channel, the mass flow rate at all bypass channel, and coolant temperature at the outlet of the reactor. PWR type reactor, at its normal operation, should not produce steam at all, in its entire fuel channel. For that reason, the desired variation that will represent the actual condition of the reactor is the variation that producing zero steam fraction at all of its fuel channels.

After the variation that represents the actual flow condition of the reactor is determined and compared with the value from the reference, the chosen variation will be used to simulate the transient condition of the reactor. Parameters that need to be observed at reactor transient condition are the system pressure, coolant mass flow rate at inlet and outlet of the reactor, temperature of fuel and cladding at all fuel channels, the temperature of the coolant at inlet and outlet of

the reactor, and steam fraction which produced inside the reactor and exiting the reactor system.

III. RESULTS AND DISCUSSION

A. Steady-State Simulation

The reactor thermal hydraulics simulation at steady-state condition has been done by varying the value of flow loss coefficient at bypass channels, and axial and radial power peaking factor. The results of this simulation on several variations are shown in Table 2.

TABLE II
STEAM FRACTION PRODUCED BY FUEL CHANNELS AT SEVERAL VARIATIONS

Power peaking factor		Flow loss coefficient	Steam fraction channel 150	Steam fraction channel 160	The steam fraction at the reactor outlet	
Axial	Radial					
1.0	1.0	0	0.467	0.371	0.085	
		4,000	0	0	0	
		8,000	0	0	0	
	1.1	0	0.484	0.370	0.085	
		4,000	0.033	0	0	
		8,000	0.025	0	0	
		12,000	0.021	0	0	
		16,000	0.018	0	0	
	1.2	0	0.494	0.368	0.085	
		4,000	0.078	0	1.10x10 ⁻⁶	
		8,000	0.067	0	6.51x10 ⁻⁷	
		12,000	0.062	0	5.00x10 ⁻⁷	
16,000		0.059	0	4.28x10 ⁻⁷		
1.3	0	0.501	0.367	0.0845		
	4,000	0.131	0	3.57x10 ⁻⁶		
	8,000	0.118	0	2.56x10 ⁻⁶		
	12,000	0.112	0	2.19x10 ⁻⁶		
	16,000	0.109	0	1.99x10 ⁻⁶		
1.1	1.0	0	0.467	0.370	0.085	
		4,000	0	0	0	
		8,000	0	0	0	
	1.1	0	0.484	0.369	0.085	
		4,000	0.017	0	0	
		8,000	0	0	0	
		0	0.493	0.368	0.085	
		4,000	0.066	0	7.31x10 ⁻⁷	
	1.2	8,000	0.055	0	3.93x10 ⁻⁷	
		12,000	0.051	0	2.86x10 ⁻⁷	
		16,000	0.048	0	2.32x10 ⁻⁷	
		0	0.502	0.367	0.085	
1.3	4,000	0.124	0	3.20x10 ⁻⁶		
	8,000	0.110	0	2.23x10 ⁻⁶		
	12,000	0.104	0	1.88x10 ⁻⁶		
	16,000	0.101	0	1.69x10 ⁻⁶		
	0	0.467	0.371	0.085		
1.2	1.0	4,000	0	0		
		8,000	0	0		
		0	0.485	0.369	0.085	
	1.1	4,000	0	0		
		8,000	0	0		
	1.2	0	0.493	0.368	0.085	
		4,000	0.055	0	4.48x10 ⁻⁷	
		8,000	0.043	0	1.88x10 ⁻⁷	
		12,000	0.037	0	0	
		16,000	0.034	0	0	
		0	0.502	0.367	0.0846	
		4,000	0.117	0	2.88x10 ⁻⁶	
1.3	8,000	0.103	0	1.94x10 ⁻⁶		
	12,000	0.096	0	1.59x10 ⁻⁶		
	16,000	0.093	0	1.41x10 ⁻⁶		
	1.3	1.0	0	0.467	0.371	0.085

1.1	4,000	0	0	0
	8,000	0	0	0
	0	0.485	0.370	0.085
	4,000	0	0	0
	8,000	0	0	0
1.2	0	0.494	0.368	0.085
	4,000	0.045	0	2.50x10 ⁻⁷
	8,000	0.029	0	0
	12,000	0.021	0	0
	16,000	0.015	0	0
1.3	0	0.502	0.367	0.085
	4,000	0.112	0	2.63x10 ⁻⁶
	8,000	0.097	0	1.71x10 ⁻⁶
	12,000	0.090	0	1.37x10 ⁻⁶
	16,000	0.086	0	1.20x10 ⁻⁶

Based on Table 2, the variation that will be used to simulate transient conditions can be determined. The desired variation is the variation of flow loss coefficient and axial and radial power peaking factor, which produce zero steam fraction at all of its fuel channels. Several variations produce zero steam fraction at all of its fuel channels. These variations are all variation with radial power peaking factor values of 1.0 and 1.1, which have a flow loss coefficient of 4,000 and 8,000, except for the variation with 1.0 axial power peaking factor value. From the result above, the chosen radial power peaking value is 1.1.

The chosen flow loss coefficient value is 8,000 because no significant mass flow rate changes that flow through the fuel channel if the flow loss coefficient value is more than 8,000. In all simulation with 8,000 flow loss coefficient value at different axial and radial power peaking factor, the maximum steam fraction generated from the fuel channel is relatively low because it is less than 12% of the coolant mass that entering the fuel channels. Determining the value of the axial power peaking factor at a normal reactor operation has to consider the power peaking factor shifting during a reactor cycle. This axial power peaking factor shifting is simulated with 1.1 radial power peaking factor value and 8,000 flow loss coefficient at bypass channels. These simulation results are shown in Table 3.

TABLE III
STEAM FRACTION PRODUCED IN THE FUEL CHANNELS AT VARIOUS AXIAL POWER PEAKING POSITION

Axial power peaking factor	Flow loss coefficient (power peaking position)	Steam fraction channel 150	Steam fraction channel 160	The steam fraction at the reactor outlet
1.1	8,000 (center)	0	0	0
	8,000 (top)	0.035	0	0
	8,000 (bottom)	0	0	0
1.2	8,000 (center)	0	0	0
	8,000 (top)	0.044	0	0
	8,000 (bottom)	0	0	0
1.3	8,000 (center)	0	0	0
	8,000 (top)	0.051	0.005	2 x 10 ⁻⁶
	8,000 (bottom)	0	0	0

Table 3 shows that the axial power peaking shift was not much affecting the steam production in the fuel channel because total heat generation in each channel remains the same. Therefore, the chosen axial power peaking factor value was assumed 1.1, the same as the radial power peaking

factor which had been chosen before. The power peaking factor with the value of 1.0 was not chosen, although it had fewer steam fraction production than 1.1 because, in actual condition, homogeneous power distribution is difficult to achieve. Thus, the parameters that were assumed to represent normal operation at steady-state conditions were a combination of 8,000 flow loss coefficient value, 1.1 radial power peaking factor value, and 1.1 axial power peaking factor value at the center of the fuel rod.

Before running simulations at transient conditions, simulation results from the chosen variation had to be verified with the value from the reference. The validation process was done by comparing coolant temperature and mass flow rate at the outlet of the reactor with the data from the reference. Operation parameters from the inlet of the reactor were not compared because those values had been used as an initial condition to run the simulation. A comparison between the value from the simulation result and the value from the reference is shown in Table 4.

It can be concluded from Table 4 that RELAP5-3D is applicable to simulate the thermal-hydraulics phenomenon in the KLT-40S reactor. The reason for the conclusion above is the small error values are shown when the simulation result is compared to the values from the reference.

TABLE IV
VERIFICATION RESULT OF KLT-40S THERMAL-HYDRAULICS MODELING WITH RELAP5-3D

Operation Parameter	Reference	Simulation	Error
Fluid temperature at reactor outlet (K)	589.15	588.645	0.086 %
Mass flow rate at reactor outlet (kg/s)	761	761.00004	$5.3 \times 10^{-6} \%$

B. Transient Simulation

The results of the fuel and its cladding temperature in the fuel channels from a transient simulation with a 10% step decrease and increase of its coolant inlet pressure are shown in Fig. 5.

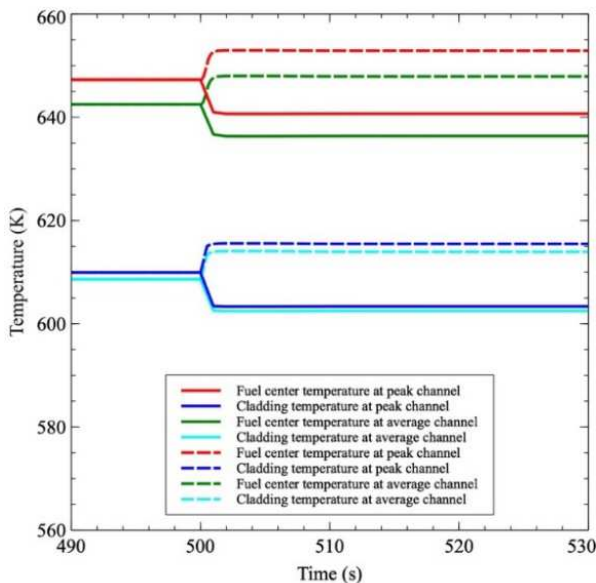


Fig. 5 Result of transient simulation with 10% step decrease and increase of the coolant inlet pressure

Fig. 5 shows that when the inlet pressure increases, the fuel and its cladding temperature will also increase because of an increase in water coolant thermal conductivity. On the contrary, when the inlet pressure decreases, fuel and its cladding will also decrease because of the decline in the water coolant thermal conductivity. At this transient condition where the inlet pressure suddenly increases to 110% and drop to 90% from its nominal value, there are no fuel and cladding temperature which have value beyond safety limit from the reference [9,13] which is 500 °C or 773.15 K for fuel material, and 2200 °F or 1437 K for cladding material. The temperature changes when the pressure decrease is more extensive than when the pressure increase. When the pressure decreases, the fuel channels will be producing steam. The appearance of steam in the fuel channel will decrease the heat transfer from the fuel into the coolant. On the other side, increasing the pressure will not producing steam in all fuel channels. Therefore it will have smaller temperatures different.

The fuel and cladding temperatures from the simulation result with a 10% ramp decrease and increase of its coolant inlet pressure are shown in Fig. 6.

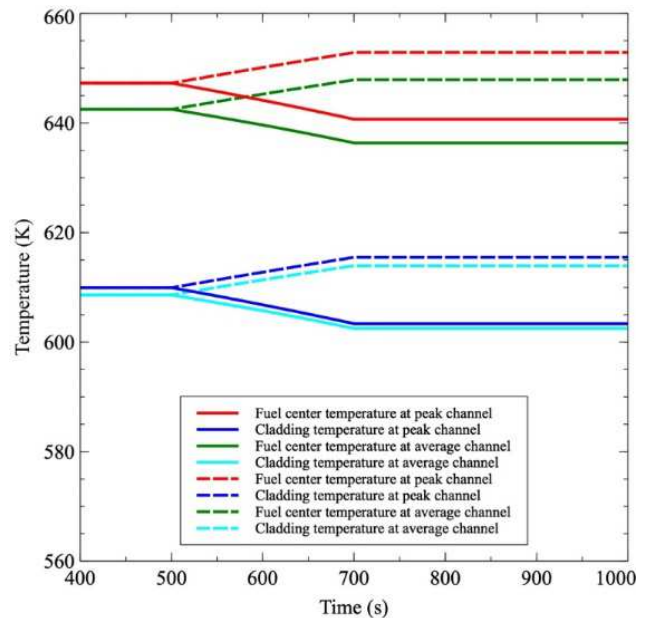


Fig. 6 Result of transient simulation with 10% ramp decrease and increase of the coolant inlet pressure

Fig.6 shows that when the pressure slowly increases, the fuel and cladding temperature will also gradually increase because of the increase in water coolant thermal conductivity. Similar behavior is also observed when the pressure slowly decreases, the fuel and cladding temperature will also decrease because of the coolant thermal conductivity changes. From Fig. 6 it can be observed that at transient condition ramp increase and decrease of its inlet pressure have similar final temperature value as in the step change of inlet pressure. In the condition where the coolant inlet pressure increase and decrease slowly 10% from its nominal value, there are no fuel and its cladding that have value beyond safety limit from the reference [9,13] which is 500 °C or 773.15 K for fuel material, and 2200 °F or 1437 K for cladding material. Fig. 7 shows the fuel and cladding

temperature at all of the fuel channels from the transient simulation result with a 20% step decrease and an increase of its coolant inlet mass flow rate.

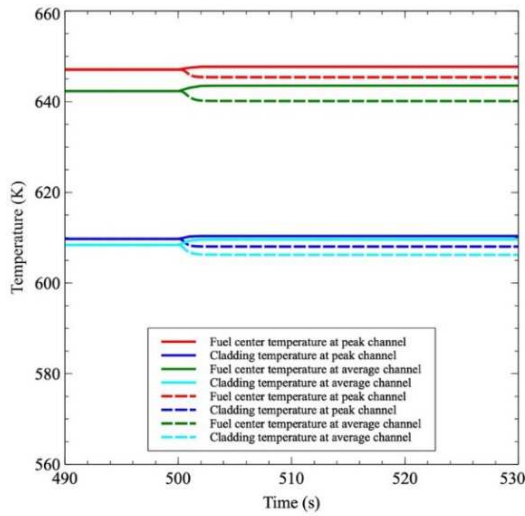


Fig. 7 Result of transient simulation with 20% step decrease and increase of the coolant inlet mass flow rate

It can be seen from Fig. 7 that the fuel and cladding temperatures at this condition do not change significantly. The increase of coolant mass flow rate at 120% from its steady value is decreasing fuel and cladding temperature but only a little. Decreasing the coolant mass flow rate will only increase the fuel and cladding temperature a little too. The fuel and cladding temperature decrease because the same amount of heat energy is transferred into the coolant that its amount has increased by 20%. The same relation happens when the coolant mass flow rate decreases 20%; the same amount of heat energy is transferred into the coolant, thus increasing the fuel and cladding temperature and producing steam in its fuel channels. In this condition, fuel, and cladding thermal safety limits are not exceeded. The fuel and cladding temperature from the simulation result with a 20% ramp decrease and increase of its inlet coolant mass flow rate is shown in Fig. 8.

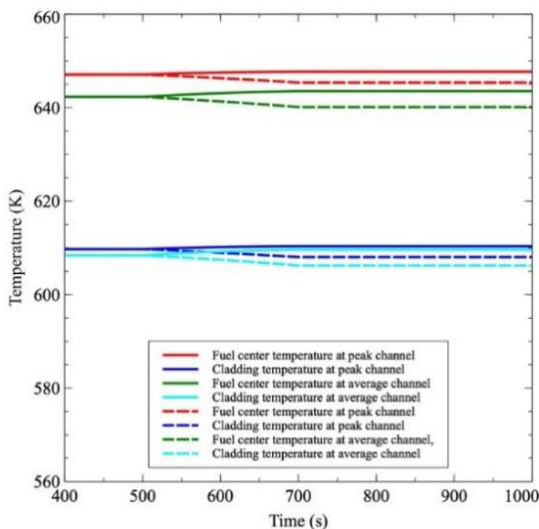


Fig. 8 Result of transient simulation with 20% ramp decrease and increase of the coolant inlet mass flow rate

It can be seen from Fig. 8 that the fuel and cladding temperature in this condition does not change much. The 20% increase in the coolant mass flow rate has little effect but slightly decreasing the temperature of the fuel and its cladding. The 20% decrease in the coolant mass flow rate is also slightly increasing the fuel and cladding temperature. The difference between ramp changes results compare to step changes results are the ramp input has smoother changes than the step input, but the final value is the same. The slight changes that happen in this ramp input simulation result have the same reason as the step input above, which is caused by the increasing and decreasing amount of water coolant that receiving the constant amount of heat energy from the fuel. When the coolant mass flow rate slowly decreases, the steam bubble will slowly begin to appear in the fuel channels. None of the fuel and cladding temperature value is passing beyond the thermal safety limit, but the interaction between steam and the cladding is not simulated in this research.

IV. CONCLUSIONS

Thermal hydraulics modeling and simulation of KLT-40S reactor at steady-state condition has been done with a chosen variation that assumed to represent the reactor normal operation condition has flow loss coefficient at bypass channels 8,000, radial power peaking power 1.1, and axial power peaking factor 1.1, positioned in the center of the fuel rod. The result of the verification is RELAP5-3D can be applied to simulate the thermal-hydraulics phenomenon of the KLT-40S reactor because its simulation result of coolant outlet temperature and mass flow rate, has a small error, less than 0.1% compared to the values from the reference. Thermal hydraulics simulation of KLT-40S reactor at transient condition has been done by increasing and decreasing the value of inlet pressure (10% from its normal value) and coolant mass flow rate (20% from its normal value) with step and ramp input. The fuel and cladding temperature value at the steady-state condition and several transient conditions are predicted in this research, and no temperature value goes beyond the safety limit.

ACKNOWLEDGMENT

This research was supported by the Department of Nuclear Engineering and Engineering Physics Faculty of Engineering, Universitas Gadjah Mada, Yogyakarta through *Dana Masyarakat UGM* of Fiscal Year 2017.

REFERENCES

- [1] "KLT-40S Overview", Advanced Reactor Information System, International Atomic Energy Agency, Vienna, 2013. Accessed from <https://aris.iaea.org/PDF/KLT-40S.pdf>, May 15, 2017.
- [2] S. M. Dmitriev *et al.*, "Computational and Experimental Investigations of the Coolant Flow in the Cassette Fissile Core of a KLT-40S Reactor," *J. Eng. Phys. Thermophys.*, vol. 90, no. 4, pp. 941–950, 2017.
- [3] S. M. Dmitriev, A. A. Barinov, A. V Varentsov, D. V Doronkov, D. N. Solntsev, and A. E. Khrobotov, "Experimental studies of local coolant hydrodynamics using a scaled model of cassette-type fuel assembly of a KLT-40S reactor," *Therm. Eng.*, vol. 63, no. 8, pp. 567–574, 2016.
- [4] A.M. Bakhmetev, I.A. Bylov, S.P. Linkov, A.V. Baklanov, I.E. Efimkina, A.G. Markelov, and Y. V. Kotikhina, "The Results of a Probabilistic Safety Analysis of the First Level of the Power Unit of

- a Floating Nuclear Thermal Power Plant with a Reactor KLT-40S”, *Atomnyye Stantsii Maloy Moshchnosti: Novoye Napravleniye Razvitiya Energetiki*, vol. 2, pp. 251-259, 2015. (in Russian)
- [5] S.S. Borodin, D.V. Doronkov, M.A. Legchanov, E.N. Polozkova, O.B. Soldatkin, V.D. Sorokin, and A.E. Khrobostov, “Design and Experimental Investigation of the Flow of Coolant in the Reactor Core Floating Power”, *Trudy Nizhegorodskogo Gosudarstvennogo Tekhnicheskogo Universiteta im. R. Alekseeva*, vol. 3, pp. 117-126, 2015. (in Russian)
- [6] A.N. Lepekhin and D.V. Kislitsyn, “Calculation Studies Severe Accident KLT-40S”, *Materialy Konferentsii KMS*, Section 1, Artikel no.16, Podolsk, March 21-22, 2012.
- [7] “RELAP5-3D Code Manual, Vol. 1-5”, The RELAP5-3D Code Development Team, Idaho National Laboratory, Idaho Falls, 2015.
- [8] V.S. Chirkin, *Database of Nuclear Material Thermophysics Properties*, Atomizdat, Moscow (1968). (in Russian)
- [9] V. V Popov *et al.*, “Results of experimental investigations for substantiation of WWER cermet fuel pin performance,” 1997.
- [10] IAEA, *Thermophysical Properties Database of Materials for Light Water Reactors and Heavy Water Reactors*, IAEA-TECDOC-1496, International Atomic Energy Agency, Vienna, 2006.
- [11] IAEA, *Accident Analysis for Nuclear Power Plants with Pressurized Water Reactors*, Safety Report Series no. 30, International Atomic Energy Agency, Vienna, 2003.
- [12] Office of Nuclear Regulatory Research (NRC), “Chapter 15 Transient and Accident Analysis,” 2005.
- [13] US Nuclear Regulatory Commission, “10 CFR 50.46 - Acceptance criteria for emergency core cooling systems for light-water nuclear power reactors,” 2010.